Transmitted, Reflected, and Converted Modes of Seismic Precursors to Shear Failure of Rock Discontinuities

El Fil, H.

Lyles School of Civil Engineering, Purdue University, West Lafayette, IN, USA

Pyrak-Nolte, L.J.

Department of Physics and Astronomy, Department of Earth, Atmospheric, and Planetary Sciences, Lyles School of Civil Engineering, Purdue University, West Lafayette, IN, USA

Bobet, A.

Lyles School of Civil Engineering, Purdue University, West Lafayette, IN, USA

ABSTRACT: The failure of rock along pre-existing discontinuities is a major concern when building structures on or in rock. A goal is to develop methodologies to identify signatures of imminent shear failure along discontinuities to enable implementation of measures to prevent the collapse of a structure. Previous studies identified precursory seismic signatures of shear failure along rock discontinuities in transmitted and reflected signals. Here, laboratory direct shear experiments were conducted on idealized saw-tooth discontinuities in gypsum to determine the differences or similarities in precursors observed in transmitted, reflected and converted elastic waves. Digital Image Correlation (DIC) was used to quantify the vertical and horizontal displacements along the discontinuity during shearing to relate the location and magnitude of slip with the measured wave amplitudes. Results from the experiments showed that seismic precursors to failure appeared as maxima in the transmitted wave amplitude and conversely as minima in the reflected amplitudes. Converted waves (S to P & P to S) were also detected and their amplitudes reached a maximum prior to shear failure. DIC results showed that slip occurred first at the top of the specimen, where the load was applied, and then progressed along the joint as the shear stress increased. This process was consistent with the precursors i.e., precursors were first recorded near the top and later at the center and finally at the bottom of the specimen. Interestingly, precursors from reflected waves were observed first, followed by precursors from transmitted and then by converted waves. Also, the differences in time of occurrence between the three precursor modes decreased along the plane of the discontinuity. The results showed that reflected waves were the most sensitive to damage and slip along a discontinuity and that monitoring for precursors may provide a method for detecting impending failure.

1. INTRODUCTION

The stability of rock structures is affected by the presence of pre-existing discontinuities such as fractures, joints and faults. It is important to study the shear strength of rock discontinuities to avoid potential failures in rock slopes and excavations along pre-existing joints. Researchers have extensively studied the shear strength of discontinuities by assessing various factors that may affect it, such as the degree of matching (Zhao, 1997), normal stress applied, surface roughness (Byerlee, 1978; Jaeger et al., 2007), whether a discontinuity is filled or unfilled (Papaliangas et al., 1993), etc. In addition to mechanically studying the shear strength of rock discontinuities, geophysical tools such as seismic monitoring have been successfully used to detect crack propagation and coalescence in Indiana Limestone samples (Modiriasari et al., 2017; 2018; 2020). Hedayat et al. (2014) employed active seismic monitoring while conducting laboratory direct shear experiments on gypsum rock samples with a single discontinuity and

detected seismic precursors—in the form of maxima in the transmitted compressional (P) and shear (S) wave amplitude prior to failure. El Fil et al., (2019) conducted similar direct shear experiments and detected the dilation and closure of a single discontinuity undergoing shear by monitoring the amplitude of transmitted elastic waves.

Recent machine learning algorithms have been developed to predict: (1) the failure time (Rouet-Leduc et al., 2017), and (2) the timing, duration and magnitude (Hulbert et al., 2019) of laboratory earthquakes obtained by conducting double direct shear experiments on joints with quartz powder, using acoustic emission data. Seismic monitoring has also been successfully employed to quantify the shear and compressional stiffness of a rock discontinuity for different loading conditions (Pyrak-Nolte et al., 1990; Choi et al., 2013; Pyrak-Nolte, 2019). According to Nakagawa et al. (2000), the transmitted and reflected compressional and shear signals do not provide enough insight into the state of stress of a discontinuity underdoing shear because it is difficult to separate the effect of normal stress from that of the shear stress during

an experiment. They conducted laboratory direct shear experiments on granite samples and were able to detect, at normal incidence to the fracture, converted waves namely, compressional (P) to shear (S) and shear (S) to compressional (P). Modiriasari et al. (2018; 2020) observed converted (S-P) signals as precursors to shear crack initiation during uniaxial experiments on Indiana limestone samples with pre-existing flaws. The existence of the converted waves was attributed to the formation of an array of oriented micro-cracks prior to coalescence.

To provide further insight into how precursors occur and the differences among precursors observed from transmitted, reflected, and converted waves, a series of direct shear experiments was conducted on a discontinuity with ideal saw-tooth asperities. The goals of the research were to: (1) monitor the shearing process of an ideal discontinuity, to compare signatures of failure in transmitted, reflected, and converted elastic waves; and (2) examine the propagation of slip as the discontinuity was driven to failure.

2. METHODOLOGY

2.1. Sample preparation

Gypsum samples were fabricated in the laboratory. Each sample was composed of two separate prismatic blocks with the following dimensions: length =152.4 mm, width= 127 mm, and thickness = 25.4 mm, as shown in Figure 1.
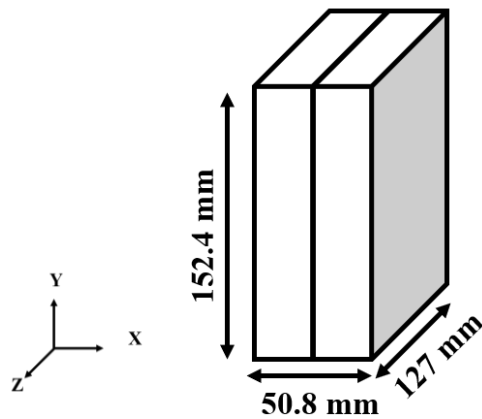

Figure 1. Schematic of the sample size

A resin mold base (Figure 2 (a)) with a saw-tooth shape was designed and 3D-printed using a Formlabs Form 2 printer. The saw-tooth had a height of 1.5 mm and an angle of 45°; as shown in Figure 2 (b).
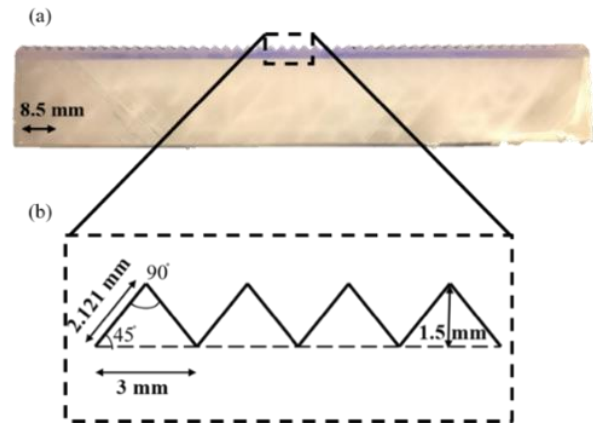

Figure 2. (a) 3D-printed resin mold base; (b) schematic of the saw-tooth geometry

The samples were prepared following a repeatable procedure (Choi, 2013; Hedayat, 2013): 11.43 g of diatomaceous earth powder was mixed with 400 cc of tap water at a rate of 54 rpm for 30 seconds. Then, 1000 g of Hydrocal B11 gypsum powder was added to the mixture and then mixed at 180 rpm for 4.5 minutes. The mixture was then poured over the mold base presented in Figure 2(b) and vibrated at high speed (100 rpm) for 5 minutes to allow the air bubbles to get to the surface. The second block was prepared in the same manner as the first, and then poured over the saw-tooth surface of the first block, after applying a water-based Dow Corning 2418 mold release emulsion agent to enable separation of the sample into two blocks after hardening.

2.2. Experimental Setup

The experimental setup is composed of a biaxial apparatus and synced ultrasonic monitoring and Digital Image Correlation (DIC) systems. A schematic of the front view of the experimental setup is shown in Figure 3(a). The sample is placed between the transducer housings (one for sources and one for receivers) in the biaxial apparatus. Each transducer housing contained a total of 9 embedded shear and compressional ultrasonic transducers with a central frequency of 1 MHz (Olympus V153RM for shear and V103RM for compressional transducers). Before shearing the sample, the transducers were coupled to the specimen for 4 hours at a normal stress of 1 MPa, using baked honey (at 90°C for 90 minutes) as a coupling agent. The biaxial apparatus included a flat jack (ENERPAC RSM500, with a capacity of 70 MPa), loading platens, steel rods, and rollers. An electronic feedback loop control (CC8 Multi-test controls machine) was used to control the flat-jack pressure to ensure that the normal load was constant throughout the experiment. All the experiments were conducted under a constant normal stress of 2 MPa. The shear stress (displacement controlled) was applied by the loading frame at a rate of 8μm/sec. While the specimen was sheared, compressional (P) and shear (S) ultrasonic waves were transmitted with a repetition rate of 100 Hz across the discontinuity and recorded.
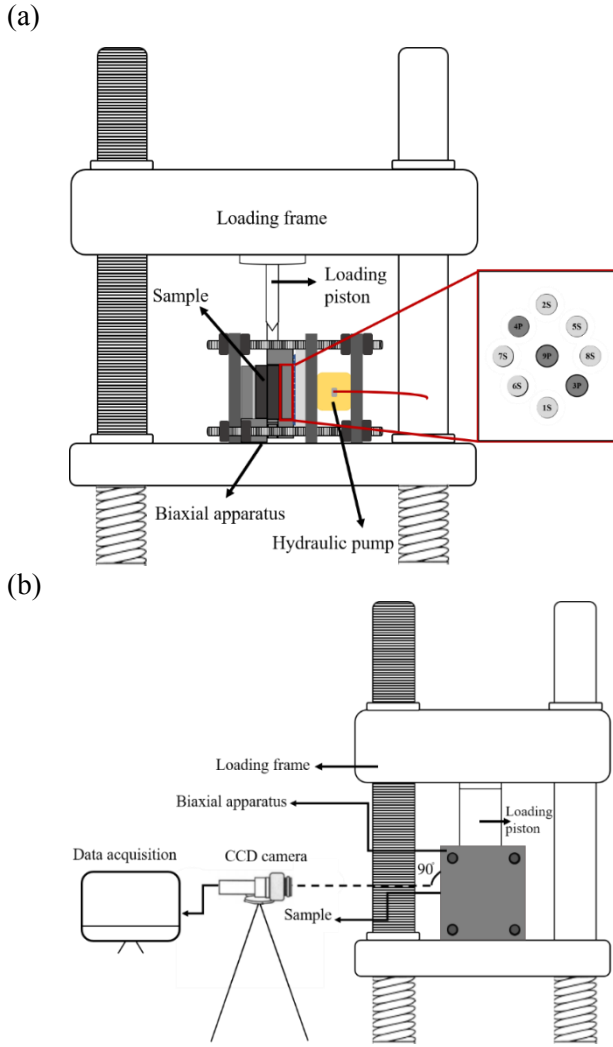
(a)

(b)

Figure 3. Schematic of the experimental setup: (a) front-view; (b) side-view showing the digital camera position with respect to the specimen.

The Digital Image Correlation system included a Grasshopper (Point Grey) CCD camera that recorded images that were 2448 by 2048 square pixels. As shown in Figure 3(b), which presents a schematic of the side view of the experimental setup, the camera was placed with its optical axis perpendicular to the surface of the specimen to minimize errors due to in-plane deformations (Pan et al., 2009). The FlyCapture® SDK software was used to control the camera and to record and save the digital images. DIC computes surface displacements by comparing recorded images before and after deformation (during the experiment). The first image recorded is used as a reference for the surface displacements. Each pixel is tracked from the reference image to all successive images of the deformed surface and the vertical and horizontal displacements are then computed.

3. RESULTS

In this section, first the results from the ultrasonic measurements during shearing are presented followed by a discussion of precursors as a function of slip initiation.

3.1. Transmitted and Reflected Signals

The normalized transmitted amplitudes from measurements with three representative transducers, namely top (2S), middle (9P), and bottom (1S) in Figure3(a), as a function of shear displacement are shown in Figure 4(a). The shear stresses are also shown on the secondary y-axis in Figure 4(a). As the shear stress increased, the normalized transmitted amplitudes of all three representative transducers were observed to increase. The increase in transmitted wave amplitude is consistent with an increase in the contact area between the two fracture surfaces caused by the application of shear stress that in turn causes an increase in fracture specific stiffness. The transmitted amplitude measured by all of the transducers increased, but then it decreased prior to failure. The peak in normalized amplitude was reached prior to the peak in the shear stress, thus representing a precursor to failure similar to that observed by Hedayat et al. (2014).

The data from the reflected-wave measurements showed the opposite behavior. The normalized reflected amplitudes of signals from the three representative transducers are displayed in Figure 4(b). As the shear stress increased, the normalized amplitude from the reflected signals decreased and then reached a minimum prior to the peak shear stress. This type of minimum represents a seismic precursor to failure as manifested in reflected waves monitor over time.

After the precursory maxima (transmitted) or minima (reflected) are reached, a decrease in transmitted wave amplitude or an increase in reflected wave amplitude occurs because of damage to the asperities that reduces the specific shear stiffness of the joint. Note also in Figures 4(a) and 4(b) that the maxima of normalized transmitted amplitudes and the minima of the normalized reflected amplitudes occur close to one another, but not at the exact same time. The data show that the precursors observed in the reflected signal data arrive slightly earlier than the precursors of the transmitted signals. For example, for data from transducer 9P, the maximum of the normalized transmitted signal occurs at a shear displacement of 1.12 mm, whereas the minimum in the normalized reflected signal occurs at a shear displacement of 1.06 mm. Additional discussion on this topic is presented in section 3.3.

3.2. Converted Signals

The normalized amplitude of converted modes (P-to-S and S-to-P) captured by three representative transducers, 2S (top), 9P (middle) and 1S (bottom), are shown in Figure 4(c). The figure also shows the shear stress as a function of shear displacement. As the shear stress increased, the normalized converted wave amplitudes measured by the representative transducers increased. A maximum in the amplitude was observed prior to the peak of the shear stress. Then the amplitude was observed to

decrease with the continued application of shear stress. This maximum in the converted wave amplitude also represents a seismic precursor to failure. As shown by Nakagawa et al. (2000), converted modes exist when a discontinuity contains oriented voids. The saw-toothed samples used in this study were designed to create oriented voids with angles of 45°. As the shear stress is applied to a saw-toothed joint, the shear displacements resulted in stiffened contact on one side of a tooth and in a relaxed or no contact on the other side thereby generating oriented voids. The magnitude of the converted waves is a function of the cross-coupling stiffness of the interface and the orientation of the microcracks. As the shear stress increases, the contact area increases between the asperities from the two fracture surfaces, which in turn reduces the size of the microcracks and increases the cross-coupling stiffness of the joint, and thus increasing the amplitude of the converted waves. With continued application of shear stress, the asperities are eventually damaged and result in a reduction in the converted wave amplitude.
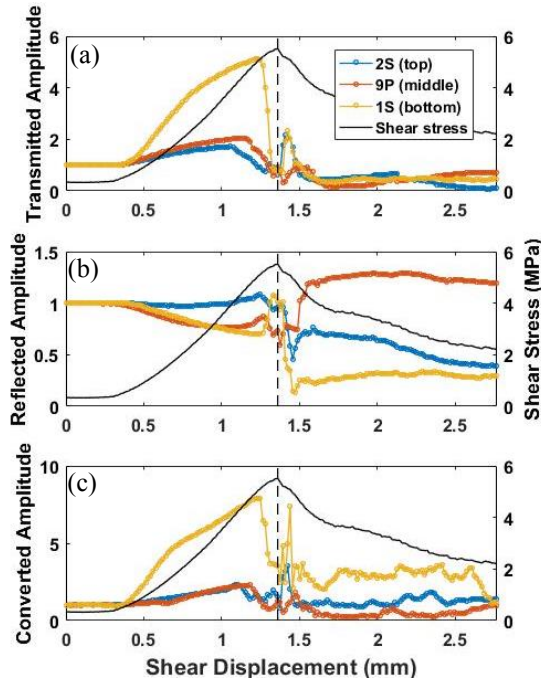

Figure 4. Normalized (a) transmitted, (b) reflected, and (c) converted wave amplitudes for three representative transducers: 2S (at top of specimen), 9P (middle) and 1S (at bottom of specimen) as a function of shear displacement. The secondary y-axis represents the shear stress.

3.3. Precursory Modes and Slip Initiation

The precursors from the normalized transmitted (maxima), converted (maxima) and reflected (minima) wave amplitudes are shown as a function of shear displacement in Figure 5 for the three representative transducers indicated by the different symbols. The top transducer (2S) was the first transducer to record all three precursors, i.e., from the transmitted, converted, and reflected waves, followed by the middle transducer (9P), and then by the bottom transducer (1S). The order here

refers to the shear displacement at which a precursor was recorded i.e., the transmitted precursor for transducer 2S was recorded at a shear displacement of 1.06 mm, which took place earlier than the transmitted precursor recorded by transducer 9P; at a shear displacement of 1.12 mm.

As discussed, the precursors indicate the onset of damage to the asperities of the joint. The results suggested that damage occurred first at the top of the specimen, followed by the middle and then the bottom. Since the shear load was applied at the top of the specimen, it was expected that slip along the discontinuity would start first at the top. This hypothesis was confirmed by monitoring slip along the discontinuity using the DIC data. Figure 5 includes snapshots of the vertical displacements recorded by the DIC camera at three elevations, at the top (y=118 m), middle (y=76 mm) and bottom (y=33 mm), for different shear stresses. At a shear stress of 3.88 MPa (70% of peak shear stress), the snapshot shows that a vertical displacement discontinuity of ~15 µm was recorded at y= 118 mm (top portion), while no significant movement was observed at y= 76 mm and 33 mm (middle and bottom portions). This is the instant when the first precursor was observed (transducer 2S) in the transmitted wave signal.

As the shear stress increased, the magnitude of slip at y=118 mm increased and, at the peak shear load (shear stress = 5.52 MPa), displacement discontinuities of ~78, 43, and 41 µm, at top, middle, and bottom of the specimen, respectively, were observed, indicating an increase in slip, and thus a propagation of slip, from the top to the bottom of the discontinuity. Finally, at a post-peak shear stress of 4.12 MPa, a large displacement discontinuity of ~ 0.53 mm was recorded at the three locations. Thus, the DIC data indicated that slip initiated from the top portion of the specimen and progressed along the discontinuity with additional shear loading. This mechanism can be thought of as a slow-motion cascade of slip failure and explains why precursory events took place progressively from the top, to the middle, and finally to the bottom of the discontinuity.

An interesting aspect is that the precursors from the reflected signals emerged first followed by those from transmitted, and finally from converted signals, indicating that reflected signals are more sensitive to the damage incurred on the discontinuity (see triangular markers in Figure 5 indicating the location and mode of precursor) and to impending failure. In addition, the difference in displacements between the appearance of each of the three precursory modes, for a given transducer, is not constant since the reflected, transmitted, and converted precursors from transducer 2S occurred at shear displacements of 0.99, 1.06, and 1.11 mm, respectively, while they were at 1.06, 1.12, and 1.14 mm, respectively, from transducer 9P and almost at the same displacement for transducer 1S.
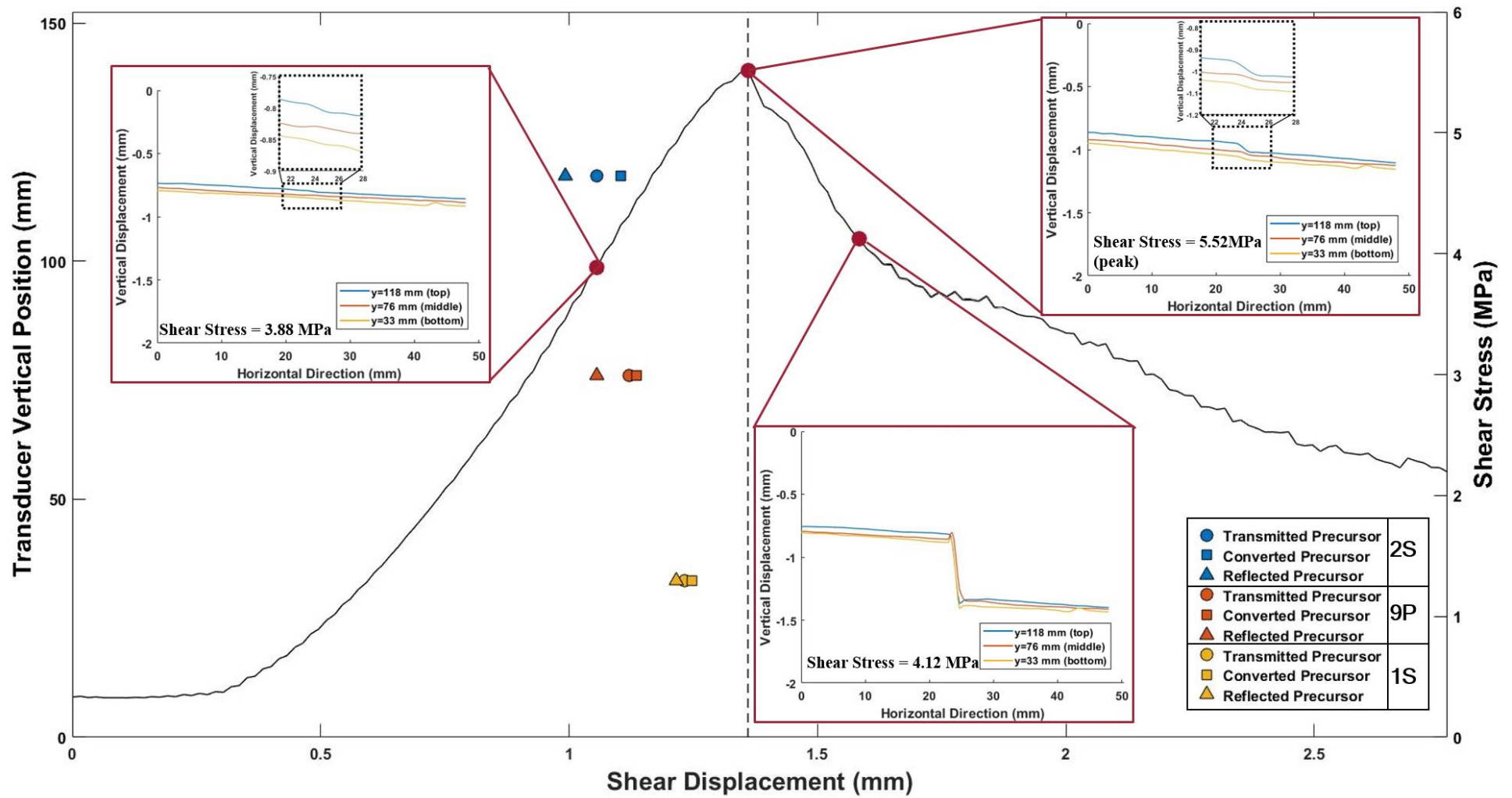
Figure 5. Transmitted (circles), reflected (triangles), and converted (squares) seismic precursors for the three representative transducers: 2S (at top of specimen), 9P (middle) and 1S (at bottom of specimen) as a function of shear displacement; also, snapshots of cross-sections of vertical displacements at various shearing stages [at 3.88, 5.52, and 4.12 MPa]

4. CONCLUSIONS

Direct shear experiments on a discontinuity with ideal saw-tooth asperities were conducted to investigate the occurrence and the mode of elastic wave precursors to shear failure. The most important outcome of the study is that seismic precursors to failure can be detected from measurements of transmitted and reflected signals, as well as from converted seismic signals. The data also show that the reflected seismic precursors emerged first, followed by the transmitted and then by the converted precursors. This indicates that reflected signals are more sensitive to shear damage than transmitted or converted signals.

Also, of note, precursors were observed first at the top of the specimen and then were progressively observed farther down the length of the discontinuity, with increasing shear load. Such an observation is consistent with the expectation of slip occurring first at the top of the specimen, where the load is applied, and propagating downwards with increasing the load. The DIC results confirmed such a relation between the first precursor, the location of the onset of slip, and the progression of precursors and slip along the discontinuity. The tests also showed that the energy partitioned between reflected, transmitted and converted signals changed with location along the discontinuity. Larger differences in time of occurrences between the three modes of precursors were observed near the top portion of the specimen, where slip first occurred, than at the bottom. This suggests that monitoring the moment when precursors are first observed may provide some information about how slip propagates along a discontinuity and about how close the discontinuity is to failure.

ACKNOWLEDGEMENTS

5. REFERENCES

1. Barton, N., & Choubey, V. (1977). The shear strength of rock joints in theory and practice. Rock Mechanics Felsmechanik Mécanique Des Roches. https://doi.org/10.1007/BF01261801

2. Byerlee, J. (1978). Friction of rocks. Pure and Applied Geophysics PAGEOPH. https://doi.org/10.1007/BF00876528

3. Choi, M.-K. (2013). Characterization of Fractures Subjected to Normal and Shear Stress. Ph.D. Thesis, Lyles School of Civil Engineering, Purdue University. ProQuest.

4. Choi, M. K., Bobet, A., & Pyrak-Nolte, L. J. (2013). The effect of surface roughness and mixed-mode loading on the stiffness ratio κ x /κ z for fractures. Geophysics. https://doi.org/10.1190/GEO2013-0438.1

5. El Fil, H., Bobet, A., & Pyrak-Nolte, L. J. (2019). Mechanical and geophysical monitoring of slip along frictional discontinuities. 53rd U.S. Rock Mechanics/Geomechanics Symposium.

6. Hedayat, A. (2013). Mechanical and Geophysical Characterization of Damage in Rocks. Ph.D. Thesis, Lyles School of Civil Engineering, Purdue University. ProQuest.

7. Hedayat, A., Pyrak-Nolte, L. J., & Bobet, A. (2014). Precursors to the shear failure of rock discontinuities. Geophysical Research Letters. https://doi.org/10.1002/2014GL060848

8. Hulbert, C., Rouet-Leduc, B., Johnson, P. A., Ren, C. X., Rivière, J., Bolton, D. C., & Marone, C. (2019). Similarity of fast and slow earthquakes illuminated by machine learning. Nature Geoscience. https://doi.org/10.1038/s41561-018-0272-8

9. Jaeger, J. C., Cook, N. G. W., & Zimmerman, R. W. (2007). Fundamentals of rock mechanics - Fourth edition. In Tectonophysics. https://doi.org/10.1016/0040-1951(77)90223-2

10. Modiriasari, A., Bobet, A., & Pyrak-Nolte, L. J. (2017). Active Seismic Monitoring of Crack Initiation, Propagation, and Coalescence in Rock. Rock Mechanics and Rock Engineering. https://doi.org/10.1007/s00603-017-1235-x

11. Modiriasari, A., Bobet, A., & Pyrak-Nolte, L. J. (2020). Seismic Wave Conversion Caused by Shear Crack Initiation and Growth. Rock Mechanics and Rock Engineering. https://doi.org/10.1007/s00603-020-02079-2

12. Modiriasari, A., Pyrak-Nolte, L. J., & Bobet, A. (2018). Emergent Wave Conversion as a Precursor to Shear Crack Initiation. Geophysical Research Letters. https://doi.org/10.1029/2018GL078622

13. Nakagawa, S., Nihei, K. T., & Myer, L. R. (2000). Shear-induced conversion of seismic waves across single fractures. International Journal of Rock Mechanics and Mining Sciences. https://doi.org/10.1016/s1365-1609(99)00101-x

14. Pan, B., Qian, K., Xie, H., & Asundi, A. (2009). Two-dimensional digital image correlation for in-plane displacement and strain measurement: A review. Measurement Science and Technology. https://doi.org/10.1088/0957-0233/20/6/062001

15. Papaliangas, T., Hencher, S. R., Lumsden, A. C., & Manolopoulou, S. (1993). The effect of frictional fill thickness on the shear strength of rock discontinuities. International Journal of Rock Mechanics and Mining Sciences And. https://doi.org/10.1016/0148-9062(93)90702-F

16. Pyrak-Nolte, L. J., Myer, L. R., & Cook, N. G. W. (1990). Transmission of seismic waves across single natural fractures. Journal of Geophysical Research.
https://doi.org/10.1029/JB095iB06p08617

17. Pyrak-Nolte, L. J. (2019). Fracture specific stiffness. In Science of Carbon Storage in Deep Saline Formations: Process Coupling across Time and Spatial Scales. https://doi.org/10.1016/B978-0-12-812752-0.00014-9

18. Rouet-Leduc, B., Hulbert, C., Lubbers, N., Barros, K., Humphreys, C. J., & Johnson, P. A. (2017). Machine Learning Predicts Laboratory Earthquakes. Geophysical Research Letters. https://doi.org/10.1002/2017GL074677

19. Zhao, J. (1997). Joint surface matching and shear strength. Part A: joint matching coefficient (JMC). International Journal of Rock Mechanics and Mining Sciences & Geomechanics Abstracts. https://doi.org/10.1016/S0148-9062(96)00062-9